

# Capacity of Line-of-Sight MIMO Channels

Heedong Do  
POSTECH, Korea  
Student Member, IEEE  
Email: doheedong@postech.ac.kr

Namyoon Lee  
POSTECH, Korea  
Senior Member, IEEE  
Email: nylee@postech.ac.kr

Angel Lozano  
Univ. Pompeu Fabra (UPF), Spain  
Fellow, IEEE  
Email: angel.lozano@upf.edu

**Abstract**—We establish an upper bound on the information-theoretic capacity of line-of-sight (LOS) multiantenna channels with arbitrary antenna arrangements and identify array structures that, properly configured, can attain at least 96.6% of such capacity at every signal-to-noise ratio (SNR). In the process, we determine how to configure the arrays as a function of the SNR. At low- and high-SNR specifically, the configured arrays revert to simpler structures and become capacity-achieving.

## I. INTRODUCTION

An unrelenting trend in the evolution of wireless communications is the move to ever higher frequencies, so as to exploit ever wider bandwidths. The current frontier is at mmWave frequencies, but researchers already have their eyes set on sub-terahertz bands where new applications await, including kiosk information transfers [1], wireless backhaul [2], and wireless interconnections within datacenters [3].

Another consolidated trend is the use of multiple-input multiple-output (MIMO) techniques, which, at microwave frequencies, enable spatial multiplexing. Precisely, the rich multipath propagation often encountered at these frequencies acts as a lens that delivers a high-rank channel.

As we move up in frequency, past the mmWave realm and into sub-terahertz bands, the transmission range necessarily shrinks and the propagation becomes mostly line-of-sight (LOS). The multipath lensing effect dwindles. At the same time, because the wavelength also shrinks dramatically, it becomes possible to span a high-rank channel based only on the array apertures themselves. In particular, broadside uniform linear arrays (ULAs) can give rise to a channel with all-equal singular values, ideal for spatial multiplexing [6], provided that the antenna spacing is  $d = \sqrt{\lambda D/N}$  where  $\lambda$  is the wavelength,  $D$  the transmission range, and  $N$  the number of antennas at either end. With this so-called *Rayleigh spacing* within the ULAs, directional signals can be launched and then resolved at the receiver without cross-talk. At 300 GHz, for instance, a Rayleigh-spaced 16-antenna ULA with an LOS range of  $D = 5$  m would occupy 26.2 cm.

With spatial multiplexing as an objective, the antenna spacings that yield all-equal singular values have been determined, not only for ULAs, but for a variety of array geometries [5], [7]–[12], and the efficacy of the corresponding transmissions have been demonstrated experimentally [13]. Spatial multiplexing, though, is the optimum transmission strategy only at high SNR. At low SNR, maximizing the received power is of essence [4, ch. 5], and that demands beamforming over a

channel whose maximum singular value is as large as possible, rather than having all-equal singular values [14], [15].

The above considerations suggest that the antenna spacing within ULAs, and more generally the antenna arrangements, should depend on the SNR. As a step in this direction, [14] proposed having three distinct ULA antenna spacings as a function of the SNR. In parallel, recognizing that both spatial multiplexing and beamforming are relevant ingredients, works such as [6], [16] propounded the use of arrays-of-subarrays (AOSAs). In this paper we show how AOSAs, properly configured, become quasi-optimum from an information-theoretic standpoint at every SNR.

## II. CHANNEL MODEL

Consider an LOS channel with broadside transmit and receive arrays. The far-field complex baseband channel coefficient from the  $m$ th transmit to the  $n$ th receive antenna is

$$h_{n,m} = \frac{\sqrt{G_t G_r} \lambda}{4\pi D_{n,m}} e^{-j \frac{2\pi}{\lambda} D_{n,m}} \quad m, n = 0, \dots, N-1 \quad (1)$$

where  $D_{n,m}$  is the distance from the  $m$ th transmit antenna to the  $n$ th receive antenna while  $G_t$  and  $G_r$  are the respective antenna gains. Provided the antenna apertures are small relative to the range,  $D_{n,m} \approx D$  such that  $|h_{n,m}|$  is approximately constant across  $m$  and  $n$ . Only the phase variations need to be modeled, and this can be done via the normalized matrix

$$\mathbf{H} = \begin{bmatrix} e^{-j \frac{2\pi}{\lambda} D_{0,0}} & \dots & e^{-j \frac{2\pi}{\lambda} D_{0,N-1}} \\ \vdots & \ddots & \vdots \\ e^{-j \frac{2\pi}{\lambda} D_{N-1,0}} & \dots & e^{-j \frac{2\pi}{\lambda} D_{N-1,N-1}} \end{bmatrix}, \quad (2)$$

which, letting  $\sigma_n(\cdot)$  denote the  $j$ th singular value of a matrix, satisfies

$$\sum_{n=0}^{N-1} \sigma_n^2(\mathbf{H}) = N^2. \quad (3)$$

We define  $\mathcal{H}$  as the set of normalized matrices  $\mathbf{H}$  produced by all possible antenna arrangements that respect the broadside disposition of the arrays and the condition of apertures much smaller than  $D$ . At the receiver,

$$\text{SNR} = \frac{\lambda^2 G_t G_r P_t}{(4\pi D)^2 B N_0} \quad (4)$$

where  $P_t$  is the transmit power,  $B$  the bandwidth, and  $N_0$  the noise spectral density. For a range  $D$  and specific parameters

(wavelength, antenna gains, power, and bandwidth), the SNR becomes determined. The information-theoretic capacity of a specific channel  $\mathbf{H}$  is [4]

$$C(\mathbf{H}, \text{SNR}) = \max_{\substack{\sum_{n=0}^{N-1} p_n = \text{SNR} \\ p_n \geq 0}} \sum_{n=0}^{N-1} \log_2 \left( 1 + p_n \sigma_n^2(\mathbf{H}) \right) \\ = \sum_{n=0}^{N-1} \log_2 \left( 1 + \left[ W - \frac{1}{\sigma_n^2(\mathbf{H})} \right]^+ \sigma_n^2(\mathbf{H}) \right) \quad (5)$$

with  $W$  such that  $\sum_{n=0}^{N-1} p_n = \text{SNR}$  and  $[z]^+ = \min(0, z)$ . Achieving  $C(\mathbf{H}, \text{SNR})$  requires a precoder whose transmit directions coincide with the right singular vectors of  $\mathbf{H}$  and whose power on the  $n$ th direction is  $p_n = [W - 1/\sigma_n^2(\mathbf{H})]^+$ , as well as a linear receiver made of the left singular vectors of  $\mathbf{H}$ .

In the setting at hand, the problem of establishing the capacity broadens to that of identifying the antenna placements yielding the channel whose individual capacity is largest, i.e.,

$$C(\text{SNR}) = \max_{\mathbf{H} \in \mathcal{H}} C(\mathbf{H}, \text{SNR}). \quad (6)$$

### III. ARRAY STRUCTURES

#### A. ULAs

The most paradigmatic array structures are ULAs, for which [11]

$$h_{n,m} = e^{-j\frac{2\pi}{\lambda} \sqrt{D^2 + (nd_r - md_t)^2}} \quad (7)$$

$$\approx e^{-j2\pi \frac{D}{\lambda}} \underbrace{e^{-j\pi \frac{n^2}{\lambda D} d_r^2}}_{\text{RX phase shifts}} e^{j2\pi \frac{nm}{\lambda D} d_r d_t} \underbrace{e^{-j\pi \frac{m^2}{\lambda D} d_t^2}}_{\text{TX phase shifts}}. \quad (8)$$

The phase shifts across the transmit and receive arrays do not affect the singular values, and can be easily compensated for, hence we can concentrate on the remaining antenna-dependent term, which gives

$$\mathbf{H}_{\text{ULA}}(N, \eta) = \begin{bmatrix} e^{j2\pi\eta \frac{0 \times 0}{N}} & \dots & e^{j2\pi\eta \frac{(N-1) \times 0}{N}} \\ \vdots & \ddots & \vdots \\ e^{j2\pi\eta \frac{0 \times (N-1)}{N}} & \dots & e^{j2\pi\eta \frac{(N-1) \times (N-1)}{N}} \end{bmatrix} \quad (9)$$

where we have introduced

$$\eta = \frac{Nd_r d_t}{\lambda D} \quad (10)$$

as a parameter that compactly describes the ULA configuration. On the one hand, tight antenna spacings correspond to  $\eta \ll 1$ . On the other hand, Rayleigh antenna spacings correspond to  $\eta = 1$ , whereby

$$\mathbf{H}_{\text{ULA}}(N, 1) = \sqrt{N} \mathbf{F}_N^* \quad (11)$$

with  $\mathbf{F}_N$  an  $N \times N$  Fourier matrix and  $\sigma_n^2(\mathbf{H}_{\text{ULA}}) = N$  for  $n = 0, \dots, N-1$ . The singular vectors of  $\mathbf{H}_{\text{ULA}}(N, 1)$  correspond to spherical waves, orthogonal when launched from the transmitter and orthogonal at the receiver.

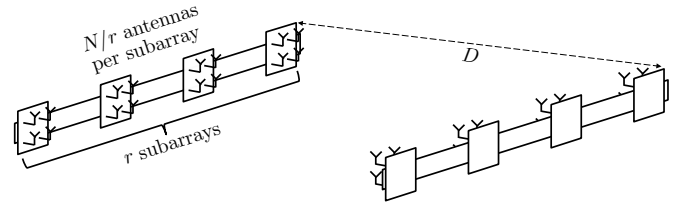


Fig. 1. AOSA featuring  $r$  subarrays, each with  $N/r$  tightly packed antennas.

#### B. Uniform AOSAs

A uniform AOSA, illustrated in Fig. 1, consists of  $r$  uniformly spaced subarrays, each with  $N/r$  tightly packed antennas [6], [17]. As the subarrays compose a ULA with configuration  $\eta$  while each subarray is compact, the channel equals the Kronecker product of  $\mathbf{H}_{\text{ULA}}(r, \eta)$  with an all-ones matrix, namely,

$$\mathbf{H}_{\text{AOSA}}(r, \eta, N/r) = \mathbf{H}_{\text{ULA}}(r, \eta) \otimes \mathbf{1}_{\frac{N}{r} \times \frac{N}{r}}, \quad (12)$$

which reverts to a tight array for  $r = 1$  and to  $\mathbf{H}_{\text{ULA}}$  for  $r = N$ . For Rayleigh subarray spacings specifically,  $\eta = 1$  and, applying (38),

$$\mathbf{H}_{\text{AOSA}} = \sqrt{r} \mathbf{F}_r^* \otimes \mathbf{1}_{\frac{N}{r} \times \frac{N}{r}} \quad (13)$$

$$= (\sqrt{r} \mathbf{I}_r \mathbf{F}_r^*) \otimes \left( \mathbf{1}_{\frac{N}{r} \times 1} \mathbf{1}_{1 \times \frac{N}{r}} \right) \quad (14)$$

$$= \left( \mathbf{I}_r \otimes \mathbf{1}_{\frac{N}{r} \times 1} \right) \sqrt{r} \left( \mathbf{F}_r^* \otimes \mathbf{1}_{1 \times \frac{N}{r}} \right) \quad (15)$$

$$= \underbrace{\left( \sqrt{\frac{r}{N}} \mathbf{I}_r \otimes \mathbf{1}_{\frac{N}{r} \times 1} \right)}_{\mathbf{U}} \frac{N}{\sqrt{r}} \mathbf{I}_r \underbrace{\left( \sqrt{\frac{r}{N}} \mathbf{F}_r^* \otimes \mathbf{1}_{1 \times \frac{N}{r}} \right)}_{\mathbf{V}^*}$$

where we have used  $(\mathbf{A}\mathbf{B}) \otimes (\mathbf{C}\mathbf{D}) = (\mathbf{A} \otimes \mathbf{C})(\mathbf{B} \otimes \mathbf{D})$ . It can be verified that  $\mathbf{U}^* \mathbf{U} = \mathbf{I}_r$  and  $\mathbf{V} \mathbf{V}^* = \mathbf{I}_N$ , indicating that the columns of  $\mathbf{U}$  and  $\mathbf{V}$  give the left and right singular vectors of  $\mathbf{H}_{\text{AOSA}}$  and that there are  $r$  nonzero singular values with  $\sigma_n^2 = N^2/r$  for  $n = 0, \dots, r-1$ .

### IV. CAPACITY UPPER BOUND

We begin by establishing an upper bound on the capacity over all possible placements of  $N$  antennas, a technical result that provides a benchmark for any achievable scheme. As detailed in Appendix A, letting

$$\rho(\text{SNR}) = \begin{cases} 1 & \text{SNR} < \zeta_1 \\ 2 & \zeta_1 \leq \text{SNR} < \zeta_2 \\ 3 & \zeta_2 \leq \text{SNR} < \zeta_3 \\ \vdots & \\ N & \zeta_{N-1} \leq \text{SNR} \end{cases} \quad (16)$$

with  $\zeta_n$  a threshold equal to the unique positive solution of

$$f\left(\frac{N^2}{n^2} \zeta_n\right) = f\left(\frac{N^2}{(n+1)^2} \zeta_n\right) \quad (17)$$

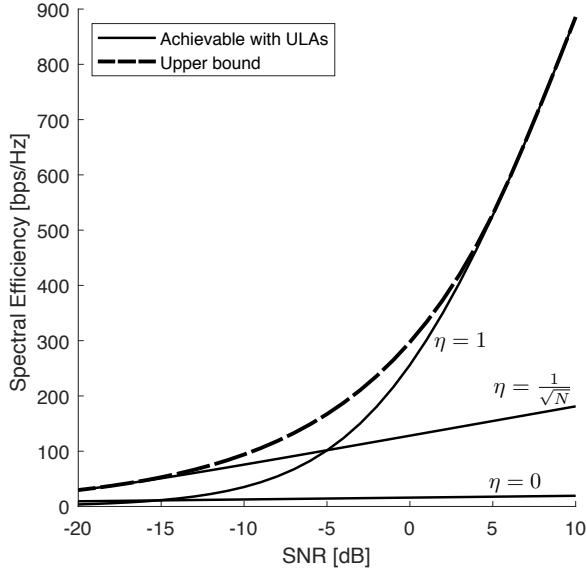


Fig. 2. Spectral efficiencies of ULAs with  $\eta = 0, 1/\sqrt{N}$ , and 1, for  $N = 256$ . Also shown is the capacity upper bound.

given the function

$$f(x) = \frac{1}{\sqrt{x}} \log_2(1+x), \quad (18)$$

we have that

$$C(\text{SNR}) \leq \rho(\text{SNR}) \log_2 \left( 1 + \frac{N^2}{\rho(\text{SNR})^2} \text{SNR} \right). \quad (19)$$

By relaxing  $\rho$  into a real-valued parameter, a slightly looser upper bound can be obtained in explicit form, precisely

$$C(\text{SNR}) \leq \begin{cases} \log_2(1 + N^2 \text{SNR}) & \text{SNR} < c/N^2 \\ N \sqrt{\frac{\text{SNR}}{c}} \log_2(1 + c) & c/N^2 \leq \text{SNR} < c \\ N \log_2(1 + \text{SNR}) & \text{SNR} \geq c \end{cases} \quad (20)$$

with  $c = -1 - 2/W_0(-2/e^2) \approx 3.92$ , given  $W_0(\cdot)$  as the principal branch of a Lambert W function.

## V. PERFORMANCE OF CONFIGURED ULAS

ULAs adopting three SNR-based configurations were proposed in [14], namely  $\eta = 0$  for low SNRs,  $\eta = 1/\sqrt{N}$  for medium SNRs, and  $\eta = 1$  for high SNRs. Shown in Fig. 2 are the spectral efficiencies of these configurations for  $N = 256$ , computed via (5) and (9), alongside the capacity upper bound. The approach is seen to be very effective at very low and at high SNR, less so elsewhere. At  $\text{SNR} = -5$  dB, for instance, only about 55% of the upper bound is attained.

By releasing  $\eta$  and allowing it to take any value in  $[0, 1]$ , the upper bound can be hugged very closely (see Fig. 3). This involves fine-tuning the antenna spacings depending on the SNR, computing the singular-value decomposition of  $\mathbf{H}_{\text{ULA}}(N, \eta)$  to obtain the precoding directions and the receiver, and solving (5) for the transmit powers.

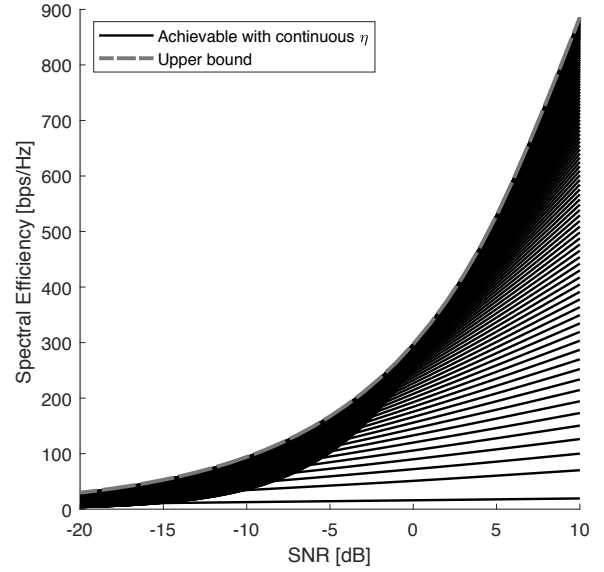


Fig. 3. Spectral efficiencies of ULAs with  $\eta \in [0, 1]$  for  $N = 256$ . Also shown is the capacity upper bound.

## VI. PERFORMANCE OF CONFIGURED AOSAS

Now, consider AOSAs with Rayleigh subarray spacings spawning the channel  $\mathbf{H}_{\text{AOSA}}(r, 1, N/r)$ . The number of antennas is  $N = 2^\ell$  with  $\ell$  integer, such that the number of subarrays  $r$  can be any power of two between 1 and  $2^\ell$ , and for each value the subarrays are balanced at  $2^\ell/r$  antennas. Then,  $\sigma_n^2 = 2^{2\ell}/r$  for  $n = 0, \dots, r-1$  and

$$C(\mathbf{H}_{\text{AOSA}}, \text{SNR}) = r \log_2 \left( 1 + \frac{2^{2\ell}}{r^2} \text{SNR} \right) \quad (21)$$

achieved by the power allocation  $p_n = \text{SNR}/r$  for  $n = 0, \dots, r-1$ . Over all possible configurations,

$$C^{\text{AOSA}}(\text{SNR}) = \max_{r \in \{1, 2, \dots, 2^\ell\}} r \log_2 \left( 1 + \frac{2^{2\ell}}{r^2} \text{SNR} \right) \quad (22)$$

$$= \max_{r \in \{1, 2, \dots, 2^\ell\}} 2^\ell f \left( \frac{2^{2\ell}}{r^2} \text{SNR} \right) \quad (23)$$

with  $f(\cdot)$  as defined in (17). Since  $f(\cdot)$  is unimodal, a value  $r$  is optimum if it is better than its adjacent brethren,  $r/2$  and  $2r$ . The SNR range over which  $r$  is better than  $r/2$  and  $2r$  is delimited by the solutions to

$$f \left( \frac{2^{2\ell}}{r^2} \text{SNR} \right) = f \left( \frac{2^{2\ell}}{(r/2)^2} \text{SNR} \right) \quad (24)$$

and

$$f \left( \frac{2^{2\ell}}{r^2} \text{SNR} \right) = f \left( \frac{2^{2\ell}}{(2r)^2} \text{SNR} \right), \quad (25)$$

which can be verified to be, respectively,  $\text{SNR} = 2^{1-2\ell} r^2$  and  $\text{SNR} = 2^{3-2\ell} r^2$ . Therefore,

$$C^{\text{AOSA}}(\text{SNR}) = r(\text{SNR}) \log_2 \left( 1 + \frac{2^{2\ell}}{r(\text{SNR})^2} \text{SNR} \right) \quad (26)$$

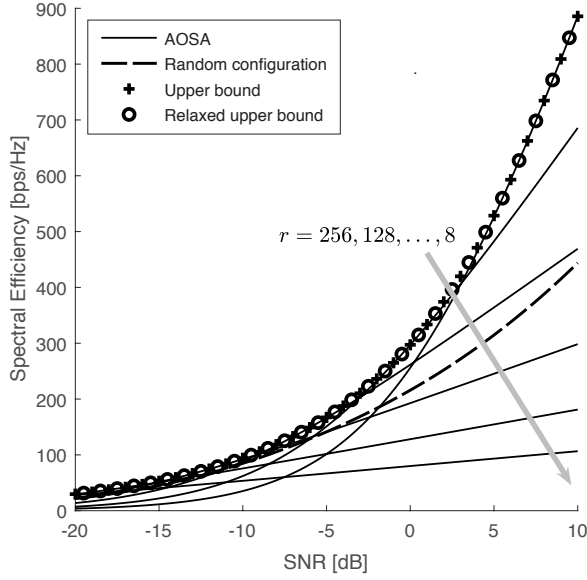


Fig. 4. Spectral efficiencies of configured AOSAs for  $N = 256$ . Also shown is the upper bound, and its relaxed version, as well as the average capacity with random antenna arrangements.

where

$$r(\text{SNR}) = \begin{cases} 1 & \text{SNR} < 2^{3-2\ell} \\ 2 & 2^{3-2\ell} \leq \text{SNR} < 2^{5-2\ell} \\ 4 & 2^{5-2\ell} \leq \text{SNR} < 2^{7-2\ell} \\ \vdots & \\ 2^\ell & 2 \leq \text{SNR} \end{cases} \quad (27)$$

indicates how the AOSAs should be configured, depending on the SNR. We note that:

- The configuration does not depend on  $N$ .
- Beyond  $\text{SNR} = 3$  dB, the AOSAs revert to ULAs.

Armed with the upper bound in Section IV, we can now gauge the optimality of configured AOSAs. It is shown in Appendix B that the gap to capacity is, in relative terms,

$$\frac{C(\text{SNR}) - C^{\text{AOSA}}(\text{SNR})}{C(\text{SNR})} \leq 1 - \frac{\sqrt{c/2}}{\log_2(1+c)} \log_2 3 \quad (28)$$

$$\approx 0.034, \quad (29)$$

meaning that AOSAs can reach, at least, 96.6% of capacity.

Shown in Fig. 4 is the spectral efficiency achievable with configured AOSAs at  $N = 256$ . The envelope of the curves for  $r = 8, 16, \dots, 256$  indeed tracks the upper bound very closely at all SNRs. The figure also shows the average capacity that would be achieved if the  $N$  antennas were randomly arranged, at transmitter and receiver, within the respective apertures (of size corresponding to ULAs with Rayleigh spacings). The optimization of the antenna placements is seen to pay off handsomely at medium and high SNRs, and effecting such optimization via AOSAs is quasi-optimum.

#### A. Low- and High-SNR Regimes

For  $\text{SNR} \leq 8/N^2$ , AOSAs reduce to single arrays with  $N$  tightly packed antennas and the ensuing  $C^{\text{AOSA}}(\text{SNR})$  for  $r = 1$  meets the upper bound in (19), indicating that

$$C^{\text{AOSA}}(\text{SNR}) = C(\text{SNR}) = \log_2(1 + N^2 \text{SNR}) \quad (30)$$

$$= N^2 \text{SNR} \log_2 e + \mathcal{O}(\text{SNR}^2). \quad (31)$$

In contrast, Rayleigh-spaced ULAs would achieve

$$C^{\text{ULA}}(\text{SNR}) = N \log_2(1 + \text{SNR}) \quad (32)$$

$$= N \text{SNR} \log_2 e + \mathcal{O}(\text{SNR}^2). \quad (33)$$

An  $N$ -fold improvement is obtained in low-SNR capacity, relative to ULAs designed for high-SNR operation.

For  $\text{SNR} \geq c$ , AOSAs reduce to ULAs and  $C^{\text{AOSA}}(\text{SNR})$  for  $r = N$  meets the relaxed upper bound in (20), indicating that

$$C^{\text{AOSA}}(\text{SNR}) = C(\text{SNR}) = N \log_2(1 + \text{SNR}) \quad (34)$$

$$= N \log_2 \text{SNR} + \mathcal{O}(1). \quad (35)$$

In contrast, tightly packed arrays would achieve

$$C^{\text{pack}}(\text{SNR}) = \log_2(1 + N^2 \text{SNR}) \quad (36)$$

$$= \log_2 \text{SNR} + \mathcal{O}(1). \quad (37)$$

An  $N$ -fold improvement is again obtained, this time by virtue of spatial multiplexing.

#### VII. SUMMARY

Properly configured, both ULAs and AOSAs are quasi-optimal for LOS transmissions. However, the latter exhibit implementational advantages:

- As opposed to  $N$ , only  $r$  radio-frequency chains are needed, one per subarray. Within each subarray, analog phase shifting can be applied.
- As opposed to  $N \times N$ , the precoder applied to every transmit symbol takes the form of an  $r \times r$  matrix.

#### ACKNOWLEDGMENT

H. Do and N. Lee are supported by the Samsung Research Funding & Incubation Center of Samsung Electronics under Project SRFC-IT1702-04. Prof. Lozano is supported by the European Research Council under the H2020 Framework Programme/ERC grant agreement 694974, and by MINECO's Projects RTI2018-102112 and RTI2018-101040.

#### APPENDIX A

Combining (5) and (6) we obtain, as starting point,

$$C = \max_{\substack{\sum_{n=0}^{N-1} \sigma_n^2 = N^2 \\ \sigma_n^2 \geq 0}} \max_{\substack{\sum_{n=0}^{N-1} p_n = \text{SNR} \\ p_n \geq 0}} \sum_{n=0}^{N-1} \log_2(1 + \sigma_n^2 p_n). \quad (38)$$

Defining

$$\bar{\sigma}_n^2 = \frac{\sigma_n^2/N^2 + p_n/\text{SNR}}{2} N^2 \quad (39)$$

$$\bar{p}_n = \frac{\sigma_n^2/N^2 + p_n/\text{SNR}}{2} \text{SNR}, \quad (40)$$

we have that the argument of (38) satisfies, by virtue of the inequality between the arithmetic and geometric means,

$$\begin{aligned} \sum_{n=0}^{N-1} \log_2(1 + \sigma_n^2 p_n) &\leq \sum_{n=0}^{N-1} \log_2 \left( 1 + \frac{N^2 \text{SNR}}{2} \left( \frac{\sigma_n^2}{N^2} + \frac{p_n}{\text{SNR}} \right)^2 \right) \\ &= \sum_{n=0}^{N-1} \log_2(1 + \bar{\sigma}_n^2 \bar{p}_n) \end{aligned} \quad (41)$$

under constraints that are preserved, namely  $\sum_{n=0}^{N-1} \bar{\sigma}_n^2 = N^2$  and  $\sum_{n=0}^{N-1} \bar{p}_n = \text{SNR}$ . From the relationship  $\bar{\sigma}_n^2 = \frac{N^2}{\text{SNR}} \bar{p}_n$ ,

$$C \leq \max_{\substack{\sum_{n=0}^{N-1} \bar{p}_n = \text{SNR} \\ \bar{p}_n \geq 0}} \sum_{n=0}^{N-1} \log_2 \left( 1 + \frac{N^2}{\text{SNR}} \bar{p}_n^2 \right). \quad (42)$$

The solution  $\bar{p}_0, \dots, \bar{p}_{N-1}$  satisfies the KKT conditions

$$\frac{2 \frac{N^2}{\text{SNR}} \bar{p}_n}{1 + \frac{N^2}{\text{SNR}} \bar{p}_n^2} + \mu_n + \lambda = 0 \quad \text{and} \quad \sum_{n=0}^{N-1} \bar{p}_n = \text{SNR} \quad (43)$$

with  $\bar{p}_n \geq 0$ ,  $\mu_n \geq 0$ , and  $\mu_n \bar{p}_n = 0$ . For  $n$  such that  $\bar{p}_n > 0$ , therefore,  $\mu_n$  should be zero and (43) can be rewritten as

$$\frac{\lambda N^2}{\text{SNR}} \bar{p}_n^2 + 2 \frac{N^2}{\text{SNR}} \bar{p}_n + \lambda = 0. \quad (44)$$

This is a quadratic equation, solved (from Vieta's formula) by two values  $\bar{p}_1$  and  $\bar{p}_2$  satisfying  $\bar{p}_1 \bar{p}_2 = \frac{\text{SNR}}{N^2}$ . The combination  $\bar{p}_0, \dots, \bar{p}_{N-1}$  that maximizes (42) therefore has the form

$$\underbrace{\bar{p}_0 = \dots = \bar{p}_{k-1}}_{=\bar{p}_1} \geq \underbrace{\bar{p}_k = \dots = \bar{p}_{r-1}}_{=\bar{p}_2} > \underbrace{\bar{p}_r = \dots = \bar{p}_{N-1}}_{=0} \quad (45)$$

where  $k\bar{p}_1 + (r-k)\bar{p}_2 = \text{SNR}$ ; the argument of (42) becomes

$$k \log_2 \left( 1 + \frac{N^2}{\text{SNR}} \bar{p}_1^2 \right) + (r-k) \log_2 \left( 1 + \frac{N^2}{\text{SNR}} \bar{p}_2^2 \right). \quad (46)$$

Assume that  $\bar{p}_1 \neq \bar{p}_2$ ,  $k \geq 1$ , and  $r-k \geq 1$ . Then, from

$$\log_2(1+x^2) + \log_2 \left( 1 + \frac{1}{x^2} \right) \leq 2 \log_2 \left( 1 + \left( \frac{x + \frac{1}{x}}{2} \right)^2 \right)$$

with equality if and only if  $x = 1$  and inequality for  $x > 0$ , and from the fact that  $\frac{N^2}{\text{SNR}} \bar{p}_1^2 \cdot \frac{N^2}{\text{SNR}} \bar{p}_2^2 = 1$ ,

$$\begin{aligned} &k \log_2 \left( 1 + \frac{N^2}{\text{SNR}} \bar{p}_1^2 \right) + (r-k) \log_2 \left( 1 + \frac{N^2}{\text{SNR}} \bar{p}_2^2 \right) \\ &< (k-1) \log_2 \left( 1 + \frac{N^2}{\text{SNR}} \bar{p}_1^2 \right) + (r-k-1) \log_2 \left( 1 + \frac{N^2}{\text{SNR}} \bar{p}_2^2 \right) \\ &\quad + 2 \log_2 \left( 1 + \frac{N^2}{\text{SNR}} \left( \frac{\bar{p}_1 + \bar{p}_2}{2} \right)^2 \right). \end{aligned} \quad (47)$$

The right-hand side of (47) is the evaluation of (42) at

$$\begin{aligned} &\underbrace{\bar{p}_0 = \dots = \bar{p}_{k-2}}_{=\bar{p}_1} > \underbrace{\bar{p}_{k-1} = \bar{p}_k}_{=\frac{\bar{p}_1 + \bar{p}_2}{2}} \\ &> \underbrace{\bar{p}_{k+1} = \dots = \bar{p}_{r-1}}_{=\bar{p}_2} > \underbrace{\bar{p}_r = \dots = \bar{p}_{N-1}}_{=0}, \end{aligned} \quad (48)$$

which contradicts (45). For the remaining cases, i.e.,  $\bar{p}_1 = \bar{p}_2$ ,  $k = 0$  or  $r-k = 0$ , all positive  $\bar{p}_n$  are identical, giving (19).

## APPENDIX B

Considering  $\text{SNR} \in [2^{-2\ell+1}, 2^3] \supset [c/2^{2\ell}, c]$  suffices since, as argued in Section VI-A, the gap vanishes elsewhere. The bound on the relative gap follows from

$$\begin{aligned} &\min_{0 \leq k \leq \ell} \left( \min_{2^{-2k+1} \leq \text{SNR} \leq 2^{-2k+3}} \frac{C^{\text{AOSA}}(\text{SNR})}{C(\text{SNR})} \right) \\ &\geq \min_{0 \leq k \leq \ell} \left( \min_{2^{-2k+1} \leq \text{SNR} \leq 2^{-2k+3}} \frac{2^{\ell-k} \log_2(1 + 2^{2k} \text{SNR})}{2^\ell \sqrt{\frac{\text{SNR}}{c}} \log_2(1+c)} \right) \\ &= \frac{\sqrt{c}}{\log_2(1+c)} \min_{0 \leq k \leq \ell-1} \left( \min_{2 \leq 2^{2k} \text{SNR} \leq 8} \frac{\log_2(1 + 2^{2k} \text{SNR})}{\sqrt{2^{2k} \text{SNR}}} \right) \\ &= \frac{\sqrt{c}}{\log_2(1+c)} \min_{2 \leq x \leq 8} \frac{\log_2(1+x)}{\sqrt{x}} = \frac{\sqrt{c}}{\log_2(1+c)} \frac{\log_2 3}{\sqrt{2}}. \end{aligned}$$

## REFERENCES

- [1] H. Song, H. Hamada, and M. Yaita, "Prototype of KIOSK data downloading system at 300 GHz: Design, technical feasibility, and results," *IEEE Commun. Mag.*, vol. 56, no. 6, pp. 130–136, Jun. 2018.
- [2] S. Hur, D. J. Kim, D. J. Love, J. V. Krogmeier, T. A. Thomas, and A. Ghosh, "Millimeter wave beamforming for wireless backhaul and access in small cell networks," *IEEE Trans. Commun.*, vol. 61, no. 10, pp. 4391–4403, Oct. 2013.
- [3] D. Halperin, S. Kandula, J. Padhye, P. Bahl, and D. Wetherall, "Augmenting data center networks with multi-gigabit wireless links," in *Proc. ACM SIGCOMM Comput. Commun. Rev.*, Aug. 2011, pp. 38–49.
- [4] R. W. Heath, Jr. and A. Lozano, *Foundations of MIMO Communication*. Cambridge University Press, 2018.
- [5] P. F. Driessen and G. Foschini, "On the capacity formula for multiple input-multiple output wireless channels: A geometric interpretation," *IEEE Trans. Commun.*, vol. 47, no. 2, pp. 173–176, Feb. 1999.
- [6] E. Torkildson, U. Madhow, and M. Rodwell, "Indoor millimeter wave MIMO: Feasibility and performance," *IEEE Trans. Wireless Commun.*, vol. 10, no. 12, pp. 4150–4160, Dec. 2011.
- [7] D. Gesbert, H. Bolcskei, D. A. Gore, and A. J. Paulraj, "Outdoor MIMO wireless channels: Models and performance prediction," *IEEE Trans. Commun.*, vol. 50, no. 12, pp. 1926–1934, Dec. 2002.
- [8] T. Haustein and U. Krauger, "Smart geometrical antenna design exploiting the LOS component to enhance a MIMO system based on Rayleigh-fading in indoor scenarios," in *Proc. IEEE Personal Indoor Mobile Radio Commun.*, Sep. 2003, pp. 1144–1148.
- [9] I. Sarris and A. Nix, "Maximum MIMO capacity in line-of-sight," in *Int. Conf. Inf. Commun. Signal Process.*, Dec. 2005, pp. 1236–1240.
- [10] F. Bohagen, P. Orten, and G. Oien, "Design of optimal high-rank line-of-sight MIMO channels," *IEEE Trans. Wireless Commun.*, vol. 6, no. 4, pp. 1420–1425, Apr. 2007.
- [11] P. Larsson, "Lattice array receiver and sender for spatially orthonormal MIMO communication," in *IEEE Veh. Techn. Conf.*, May 2005.
- [12] X. Song and G. Fettweis, "On spatial multiplexing of strong line-of-sight MIMO with 3D antenna arrangements," *IEEE Wireless Commun. Lett.*, vol. 4, no. 4, pp. 393–396, Apr. 2015.
- [13] C. Sheldon, E. Torkildson, M. Seo, C.P. Yue, U. Madhow, and M. Rodwell, "A 60GHz line-of-sight 2x2 MIMO link operating at 1.2Gbps," in *IEEE AP-S Int. Symp.*, Jul. 2008.
- [14] M. Matthaiou, A. Sayeed, and J. A. Nossek, "Maximizing LoS MIMO capacity using reconfigurable antenna arrays," in *ITG Workshop on Smart Antennas (WSA)*, 2010, pp. 14–19.
- [15] N. Chiurtu and B. Rimoldi, "Varying the antenna locations to optimize the capacity of multi-antenna Gaussian channels," in *Proc. IEEE Int. Conf. Acoust. Speech Signal Process.*, Jun. 2000, pp. 3121–3123.
- [16] E. Torkildson, B. Ananthasubramaniam, U. Madhow, and M. Rodwell, "Millimeter-wave MIMO: Wireless links at optical speeds," in *Allerton Conf. Commun., Control and Computing*, 2006, pp. 1–9.
- [17] C. Lin and G. Y. Li, "Terahertz communications: An array-of-subarrays solution," *IEEE Commun. Mag.*, vol. 54, no. 12, pp. 124–131, 2016.